# Improving beampatterns of two-dimensional random arrays using convex optimization

**Peter Gerstoft**[a] **and William S. Hodgkiss**
*Marine Physical Laboratory, Scripps Institution of Oceanography, La Jolla, CA 92093-0238*
*gerstoft@ucsd.edu, wshodgkiss@ucsd.edu*

**Abstract:** Sensors are becoming ubiquitous and can be combined in arrays for source localization purposes. If classical conventional beamforming is used, then random arrays have poor beampatterns. By precomputing sensor weights, these beampatterns can be improved significantly. The problem is formulated in the frequency domain as a desired look direction, a frequency-independent transition region, and the power minimized in a rejection-region. Using this formulation, the frequency-dependent sensor weights can be obtained using convex optimization. Since the weights are data independent they can be pre-computed, the beamforming has similar computational complexity as conventional beamforming. The approach is demonstrated for real 2D arrays.


**PACS numbers:** 43.60.Fg [OG]
**Date Received:** December 31, 2010 **Date Accepted:** January 31, 2011

## 1. Introduction

Sensors are becoming ubiquitous and can be combined in arrays for source localization purposes. Random arrays or *ad hoc* arrays consist of a group of sensors clustered together where the locations are non-optimal from a beamforming perspective. The location of each senor is accurately known, but each location has been randomly selected, for example due to logistics, topography, or currents. Examples of such networks include seismics,[1–3] ocean acoustics,[5,6] air acoustics,[7,8] and speech communication applications.[9]

The sensors used here are assumed to be fixed, but for frequency domain beamforming it is possible to adjust the complex-valued weighting of each sensor to give well-defined beampatterns. While there are several methods for determining the weights, we focus on one that gives a frequency-independent main beamwidth. This can be formulated as a linearly constrained optimization problem that can be solved using convex optimization.[10] An introduction to convex optimization with beamforming can be found in Ref. 11 where robustness of adaptive beamforming[12–14] is of primary concern. Here we will apply convex optimization for data-independent beampattern optimization.

Since the locations of the sensors are known accurately, these sensors can be combined into an array of stations and used for beamforming. However, these stations are not located ideally for reducing sidelobes. Rather, the stations are placed randomly[15] or in an *ad hoc*[16] fashion. The sidelobes for such a network appear random and the beampattern has strong contributions outside the main-lobe.[15,16] Aliasing and grating lobes are due to the periodicity in a uniform array. This aliasing phenomenon is not encountered in random arrays where the sensors have no regular inter element spacing. Indeed, the average distance between the sensors is often larger than half a wavelength.

The sensor nodes are random in location, and there exists no other tools than simulation to analyze deterministic aperiodic arrays beyond a statistical characterization.[15,16] This is shown by the example in Fig. 1 for two 72 elements arrays, a random array from Cascadia (WA) [Fig. 1(a)] and a regular rectangular array with elements

[a]Author to whom correspondence should be addressed.

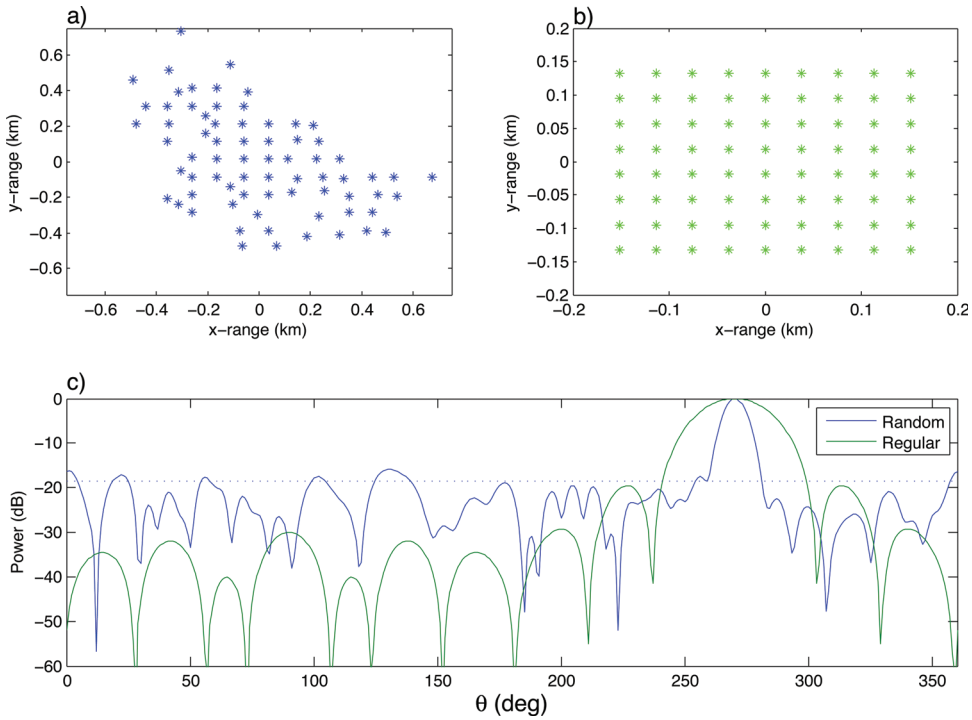


Fig. 1. (Color online) Beampattern (dB) for the random array consisting of seismic stations in Cascadia and a regular rectangular array. (a) Random array consisting of 72 stations, (b) regular array with 72 stations, and (c) beampatterns.

spaced at distance $\lambda/2$ [Fig. 1(b)]. Horizontally propagating plane waves with 3 km/s phase speed are assumed in the example. For a 270° look direction and uniform amplitude weights, the beampatterns in azimuth are shown for the regular rectangular array and the Cascadia random array [Fig. 1(c)]. Clearly, the array response from the random array does not decay with azimuth, but shows random sidelobes. Due to the larger aperture the random array has a very narrow main-lobe.

For regular arrays the spatial sampling has to be dense (i.e., $\lambda/2$ for a line array) but for random arrays there are no such limitations. In practice there is an upper limit as the coherence between elements is lost and the processing neglects velocity inhomogenities. Typically, velocity inhomogenities are not incorporated into the beamforming, but large-scale inhomogenities potentially could be incorporated.

For regularly spaced arrays both in 1D or 2D it is often possible to compute the weighting analytically[17,18] or using numerical procedure for extracting these, using simulated annealing[19] or total least squares.[9,20] For 2D random arrays, beampatterns can be improved by adaptive beamforming[21,22] parametric methods,[8] or data-independent optimization of the shading vector as demonstrated here.

## 2. Constant spatial main-lobe

The beamformer is formulated in the frequency domain and broadband results are then obtained by summing individual frequency components. In the following, a set of complex-valued weights is obtained for each look direction and frequency.

### *2.1. Signal model*

For the $N$ sensors with all sensor location concatenated in a location vector $(x, y)$, the steering vector in slowness direction $\mathbf{s} = (s_x, s_y)$ is,

$$\mathbf{a}(\mathbf{s}) = \exp(i\omega(\mathbf{x}s_x + \mathbf{y}s_y)). \quad (1)$$

The beamformer output power in desired slowness direction $\mathbf{s}_d$ is,

$$B(\mathbf{s}_d) = \mathbf{w}^H(\mathbf{s}_d)\mathbf{R}\mathbf{w}(\mathbf{s}_d), \tag{2}$$

where $\mathbf{w}$ is the weight vector and the cross-spectral density matrix $\mathbf{R} = (1/M)\sum_{m=1}^{M} \mathbf{d}_{\mathrm{obs},m}\mathbf{d}_{\mathrm{obs},m}^{\mathrm{H}}$ for $M$ observations of the data snapshot vector $\mathbf{d}_{\mathrm{obs}}$. For conventional (Bartlett) beamforming the weight vector is given by

$$\mathbf{w}(\mathbf{s}_d) = \mathbf{a}(\mathbf{s}_d)/N. \tag{3}$$

### 2.2. Convex optimization of sensor weights

At each frequency, we determine the weights $\mathbf{w}(\omega)$ by minimize the power in the rejection-region for a steering vector in desired look direction $\mathbf{s}_d$,

$$\min_{\mathbf{w}} ||(\mathbf{w}^{\mathrm{H}}\mathbf{A}_r)||_p \quad \text{subject to } \mathbf{w}^{\mathrm{H}}\mathbf{a}(\mathbf{s}_d) = 1 \quad \max[\mathbf{w}^{\mathrm{H}}\mathbf{A}_t], < 1 \tag{4}$$

where $\mathbf{A}_r$ is a matrix with each column corresponding to a steering vector for all slownesses in the rejection-region and $\mathbf{A}_t$ is a matrix of steering vectors corresponding to all slownesses in the transition region. In the present implementation, we have assumed for simplicity that the transition region in the slowness domain is a square centered at $\mathbf{s}_d$. It is easy to constrain the optimization to follow a prescribed decay in the transition region.[21] However, we have chosen not to implement this constraint but just limit the power in the transition region.

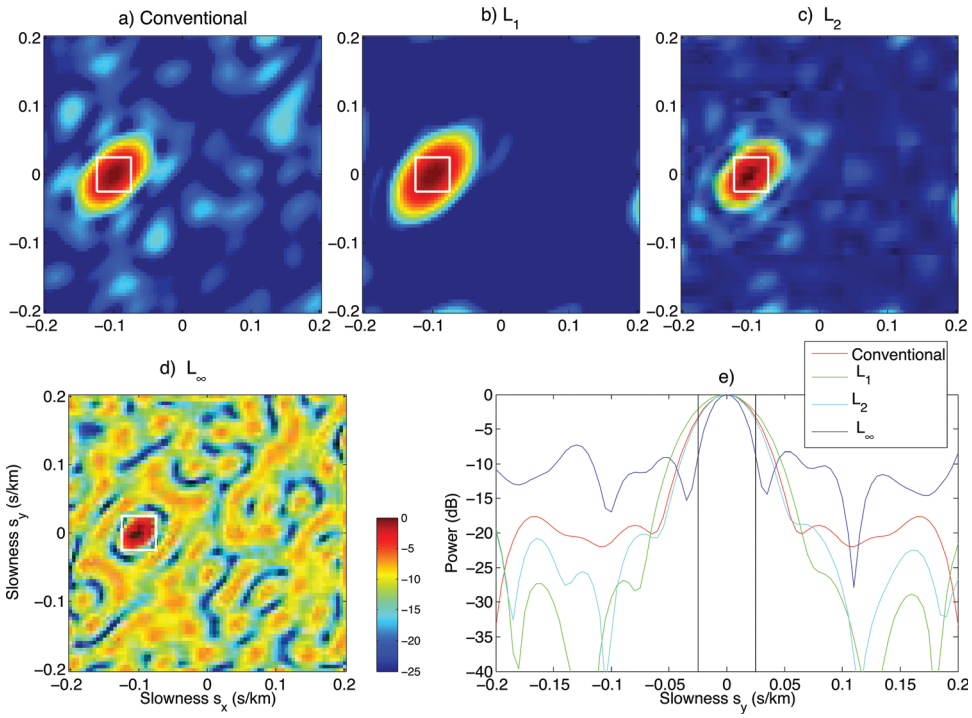


Fig. 2. (Color online) Beampattern for Cascadia array in Fig. 1 with a transition region of 0.05 s/km (square) around the look direction at $(s_x, s_y) = (-0.1, 0)$ s/km. The 2D beampattern are (a) conventional, (b) $L_1$ rejection-region, (c) $L_2$ rejection-region, and (d) $L_\infty$ rejection-region. (e) Beampatterns across $s_y$ slowness with $s_x = -0.1$ s/km for conventional, $L_1$, $L_2$, and $L_\infty$ rejection-regions.

Any norm $||\ ||_p$ can be used for solving the optimization problem in Eq. (4) and the $L_1$, $L_2$, or $L_\infty$ norms are used here. The $L_1$ norm sums the absolute values ($||\mathbf{y}||_1 = \sum_{i=1}^{m} |y_i|$) for all points in the rejection-region, whereas the $L_\infty$ norm gives the largest value ($||\mathbf{y}||_\infty = \max_{i=1,\ldots,m} |y_i|$) in the rejection-region. The $L_2$ norm ($||\mathbf{y}||_2 = \sqrt{\sum_{i=1}^{m} |y_i|^2}$) gives results in between these two norms.

The constrained optimization problem in Eq. (4) is a convex optimization problem since any norm minimization is convex and the constraints limit the search space, see Chapter 6 in Boyd and Vandenberghe.[10] This can be solved efficiently with CVX.[23,24] Note, that Eq. (4) is data-independent and can be pre-computed before any data is used in the beamforming in Eq. (2).

## 3. Example

We illustrate the 2D beamforming with an array installed to detect seismic tremor.[3,4] Seismic tremor is a continuous noise appearing with regular intervals (about 14 months in Cascadia, WA). It is believed that the noise originates from the plate boundary some 30 km below the Cascadia array and tremor typically impinges on the array with

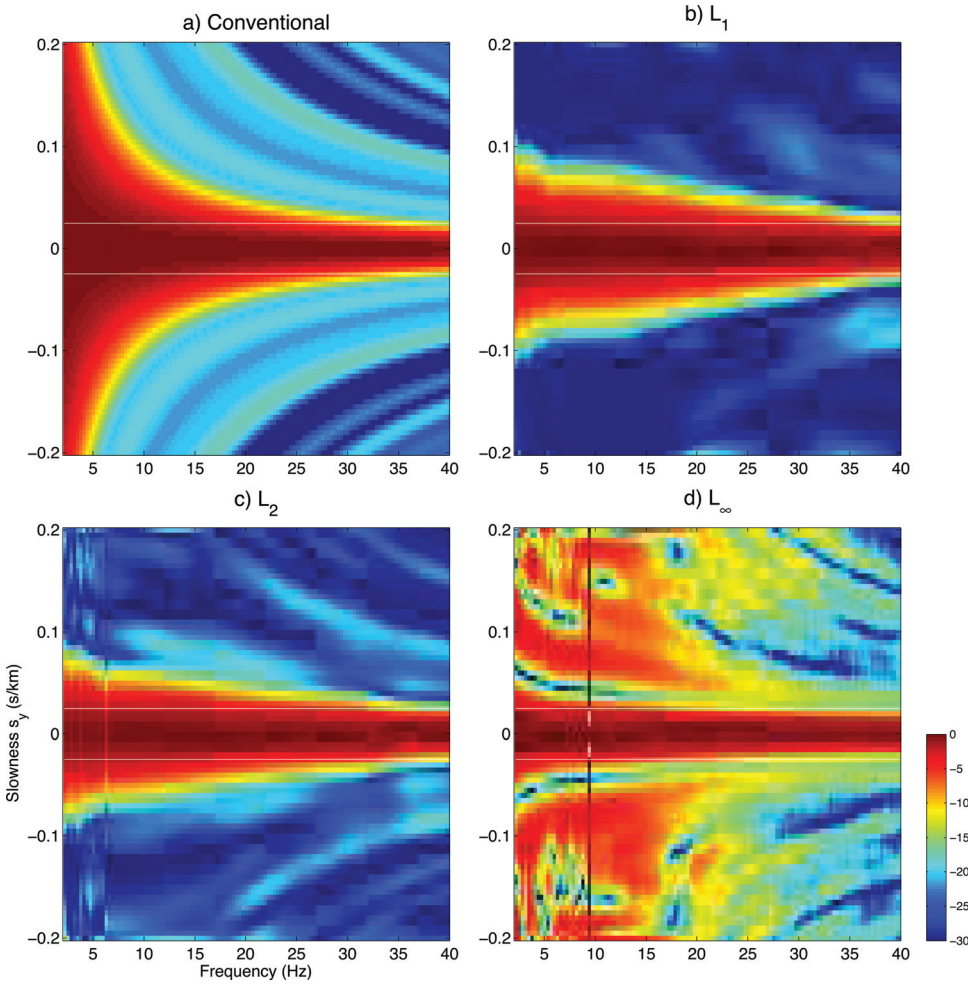


Fig. 3. (Color online) Broadband beampattern across $s_y$ slowness ($s_x = -0.1$ s/km) for the (a) conventional, (b) $L_1$ rejection-region, (c) $L_2$ rejection-region, and (d) $L_\infty$ rejection-region. Horizontal lines indicate the transition region.

phase velocities of 10 km/s (slowness 0.1 s/km). The array [Fig. 1(a)] is quite dense with 72 sensors placed within a 1.2-km square and of interest is the broadband response from 2 to 40 Hz. We initially use a frequency of 20 Hz which gives good resolution of the conventional beamformer power, Fig. 2(a).

Since the array is not regular, we apply the rejection-region algorithm to the beam response in the slowness domain, minimizing the response in the region outside the square shown in Fig. 2. The slowness domain from $-0.2$ to 0.2 s/km is gridded into $81 \times 81$ cells. The beam response is minimized in a square with sides 0.05 s/km from the look direction. For each frequency and look direction we are minimizing $81^2 - 11^2 = 6480$ equations for the 72 complex-valued sensor weights. We solve it with CVX[23,24] in about 0.5 min CPU time on a MacBook Pro.

The rejection-region formulation can be implemented using different norms as illustrated in Fig. 2. The $L_\infty$ norm (minimizing the maximum power) tends to give a relative flat rejection-region level, how flat it tends to depend on the number of elements, more elements tend to average out the fluctuations. The $L_1$ norm (minimizing the average power) does not give a flat response, but focuses on minimizing the total power in the rejection-region. Since it uses relatively more effort to reduce the sidelobes close to the look direction, the beampattern using the $L_1$ norm decays with distance from the look direction. The $L_2$ norm is a compromise between the $L_1$ and $L_\infty$ norms and it has here nearly an identical main-lobe as the conventional beamformer, but lower sidelobes. For the same size of the transition region, the $L_1$ norm gives lower rejection-region levels, but a larger main-lobe than when using the $L_\infty$ norm.

The $L_1$ norm does not have a requirement that the main-lobe should stop outside the transition region, but it can extend past the transition region. For distributed sources over a wide slowness region such as ambient noise, the $L_1$ norm might give a better representation of the source power in the look direction. For localizing a point source, the narrow constant beampattern ($L_\infty$ norm) is preferable.

We apply the rejection-region derived weights at 100 frequencies from 2 to 40 Hz as shown in Fig. 3. At 3 Hz, the array has an aperture of about $\lambda/2$. Thus, unless near field modeling is used the array does not have useful resolution below 3 Hz. The weights are not well-determined either since the individual steering vectors are too similar. As observed previously, the $L_1$ norm gives the lowest sidelobes. It is not too concerned with the width of the main-lobe and the effective width decreases as frequency increases. The $L_\infty$ norm gives a constant main-lobe.

## 4. Conclusion

A data-independent criterion for minimizing the sidelobes of 2D random arrays has been developed and demonstrated using convex optimization. Overall, the $L_1$ norm is preferred for minimizing the sidelobes in the rejection-region.

## Acknowledgments

The Office of Naval Research under Grant No. N00014-05-1-0264 supported this work.

## References and Links

[1]P. Gerstoft, M. C. Fehler, and K. G. Sabra, "When Katrina hit California," Geophys. Res. Lett. **33**, L17308 (2006).

[2]K. D. Koper and B. de Foy, "Seasonal anisotropy of short-period seismic noise recorded in south Asia," Bull. Seismol. Soc. Am. **98**, 3033–3045 (2008).

[3]A. Ghosh, J. E. Vidale, J. R. Sweet, K. C. Creager, and A. G. Wech, "Tremor patches in Cascadia revealed by seismic array analysis," Geophys. Res. Lett. **36**, L17316 (2009).

[4]J. Zhang, P. Gerstoft, P. M. Shearer, H. Yao, J. E. Vidale, H. Houston, and A. Ghosh, "Cascadia tremor spectra: Low corner frequencies and earthquake-like falloff at high frequencies," Nature (in press).

[5]W. S. Hodgkiss and V. C. Anderson, "Hardware dynamic beamforming," J. Acoust. Soc. Am. **69**, 1075 (1981).

[6]R. L. Culver and W. S. Hodgkiss, "Comparison of Kalman and least squares filters for locating autonomous very low frequency acoustic sensors," IEEE J Ocean. Eng. **13**, 282–290 (1988).
[7]T. F. Brooks and W. M. Humphreys, "A deconvolution approach for the mapping of acoustic sources (DAMAS) determined from phased microphone arrays," J. Sound Vib. **294**, 856–879 (2006).
[8]T. Yardibi, J. Li, P. Stoica, and L. N. Cattafesta, "Sparsity constrained deconvolution approaches for acoustic source mapping," J. Acoust. Soc. Am. **123**, 2631–2642 (2008).
[9]S. Doclo and M. Moonen, "Design of far-field and near-field broadband beamformers using eigenfilters," Signal Process. **83**, 2641–2673 (2003).
[10]S. P. Boyd and L. Vandenberghe, *Convex Optimization*, (Cambridge University Press, New York, 2004), Chap. 1–7.
[11]A. B. Gershman, N. D. Sidiropoulos, S. Shahbazpanahi, M. Bengtsson, and B. Ottersten, "Convex optimization-based beamforming," IEEE Signal Process. Mag. **27**, 62–75 (2010).
[12]S. A. Vorobyov, A. B. Gershman, and Z.-Q. Luo, "Robust adaptive beamforming using worst-case performance optimization: A solution to the signal mismatch problem," IEEE Trans. Signal Process. **51**, 313–324 (2003).
[13]R. G. Lorenz and S. P. Boyd, "Robust minimum variance beamforming," IEEE Trans. Signal Process. **53**, 1684–1696 (2005).
[14]Z. Xiao, W. Xu, and X. Gong, "Robust matched field processing for source localization using convex optimization," in IEEE Oceans Europe Conference (Bremen, Germany 2009).
[15]B. D. Steinberg, *Principles of Aperture and Array System Design: Including Random and Adaptive Arrays* (Wiley-Interscience, New York, 1976), Chap. 1–5.
[16]H. Ochiai, P. Mitran, H. V. Poor, and V. Tarokh, "Collaborative beamforming for distributed wireless ad hoc sensor networks," IEEE Trans. Signal Process. **53**, 4110–4124 (2005).
[17]H. L. Van Trees, *Optimum Array Processing* (Wiley, New York, 2002), Chap. 2–4.
[18]B. P. Kumar and G. R. Branner, "Generalized analytical technique for the synthesis of unequally spaced arrays with linear, planar, cylindrical or spherical geometry," IEEE Trans. Antennas Propag. **53**, 621–634 (2005).
[19]V. Murino, A. Trucco, and C. S. Regazzoni, "Synthesis of unequally spaced arrays by simulated annealing," IEEE Trans Signal Process. **44**, 119–122 (1996).
[20]M. Crocco and A. Trucco, "The synthesis of robust broadband beamformers for equally-spaced linear arrays," J. Acoust. Soc. Am. **128**, 691–701 (2010).
[21]S. Yan, C. Hou, X. Ma, and Y. Ma, "Convex optimization based time-domain broadband beamforming with sidelobe control," J. Acoust. Soc. Am. **121**, 46–49 (2007).
[22]S. Yan, Y. Ma, and C. Hou, "Optimal array pattern synthesis for broadband arrays," J. Acoust. Soc. Am. **122**, 2686–2696 (2007).
[23]M. Grant and S. Boyd, cvx, Version 1.21 Matlab Software for Disciplined Convex Programming available at http://cvxr.com/cvx (Last viewed January 25, 2011).
[24]M. Grant and S. Boyd, "Graph implementations for nonsmooth convex programs," in *Recent Advances in Learning and Control* (Springer-Verlag, Berlin, 2008), pp 95–110.